J. Membrane Biol. 168, 47–61 (1999)

The Journal of
Membrane
Biology

pH-Sensitive Gating Kinetics of the Maxi-K Channel in the Tonoplast of *Chara australis*

H. Lühring
Institut für Biologische Informationsverarbeitung, Forschungszentrum Jülich GmbH, D-52425 Jülich, Germany

Received: 8 May 1998/Revised: 18 September 1998

Abstract. The most frequently observed K^+ channel in the tonoplast of Characean giant internodal cells with a large conductance (*ca.* 170 pS; Lühring, 1986; Laver & Walker, 1987) behaves, although inwardly rectifying, like animal maxi-K channels. This channel is accessible for patch–clamp techniques by preparation of cytoplasmic droplets, where the tonoplast forms the membrane delineating the droplet. Lowering the pH of the bathing solution, that virtually mimicks the vacuolar environment, from an almost neutral level to values below pH 7, induced a significant but reversible decrease in channel activity, whereas channel conductance remained largely unaffected. Acidification (pH 5) on both sides of the membrane decreased open probability from a maximum of 80% to less than 20%. Decreasing pH at the cytosolic side inhibited channel activity cooperatively with a slope of 2.05 and a pK_a 6.56. In addition, low pH at the vacuolar face shifted the activating voltage into a positive direction by almost 100 mV. This is the first report about an effect of extraplasmatic pH on gating of a maxi-K channel. It is suggested that the *Chara* maxi-K channel possesses an S4-like voltage sensor and negatively charged residues in neighboring transmembrane domains whose S4-stabilizing function may be altered by protonation. It was previously shown that gating kinetics of this channel respond to cytosolic Ca^{2+} (Laver & Walker, 1991). With regard to natural conditions, pH effects are discussed as contributing mainly to channel regulation at the vacuolar membrane face, whereas at the cytosolic side Ca^{2+} affects the channel. An attempt was made to ascribe structural mechanisms to different states of a presumptive gating reaction scheme.

Key words: *Chara* — Gating — Ion channel — pH — Tonoplast

Correspondence to: H. Lühring

Introduction

The tonoplast of the giant green alga *Chara australis,* enclosing a large central vacuole and separating it from the cytoplasmic compartment, is equipped with several ion transport systems. Two electrogenic ion pumps, an H^+-ATPase and an H^+-pyrophosphatase (PPase) have been identified (Shimmen & MacRobbie, 1987; Takeshige, Tazawa & Hager, 1988; Takeshige & Hager, 1988). In addition, a highly selective, Ca^{2+}_{cyt}-activated and voltage-sensitive K^+ channel with a large conductance of *ca.* 170 pS (Lühring, 1986; Laver & Walker, 1987; Laver, Fairley & Walker, 1989) and a Cl^- channel of about 21 pS (Tyerman & Findlay, 1989) have been characterized. Besides, there were reports on Ca^{2+}-dependent K^+ channels of smaller conductance in the tonoplasts of several members of the *Chara* family (60 pS in *Chara corallina,* Tyerman & Findlay, 1989; 60–80 pS in *Nitellopsis obtusa,* Pottosin, 1990; 100–130 pS in *Chara gymnophylla,* Pottosin et al., 1993; although it may be suspected that these K^+ channels are subconductances of the large conductance channel due to experimental conditions). It is noteworthy that membrane voltage across the Characean tonoplast is close to the K^+ reversal voltage (Lühring, 1986). Apparently, the electrical energy gradient generated by electrogenic pumps is dissipated via those short-circuiting K^+ channels. Therefore, it appeared reasonable to look for a regulatory mechanism mitigating a waste of energy. Considering the large conductance of 170 pS and the population density of the K^+ channel (1–4 channels per μm^2), an effective regulatory mechanism appears to be inevitable. Soon after initial characterization of the high-conductance K^+ channel (Lühring, 1986; Laver & Walker, 1987), Ca^{2+} at elevated cytosolic concentration ($EC_{50} \geqslant 100\ \mu M$) was found to inhibit the activity of the channel (Laver, 1990; Laver & Walker, 1991). Ca^{2+}_{cyt} is known to be involved in the excitation process of the Characean

tonoplast (Shimmen & Nishikawa, 1988, and citations therein).

One of the first channel types studied by patch-clamp techniques was a high conductance K^+-selective channel, which has since then been referred to as BK (Marty, 1983; Blatz & Magleby, 1987) or as maxi-K channel (Latorre & Miller, 1983). Maxi-K channels show voltage-dependent kinetics and exist in both Ca^{2+}-activated and non-Ca^{2+}-activated forms. Among animal cells, they are ubiquitous and are believed to play a role in membrane excitability and excretion (Latorre & Miller, 1983; Blatz & Magleby, 1987). Similar 'maxi-K' channels have not been identified to date in any plant cells other than those of Charophytes (Laver et al., 1989) and, possibly, of *Acetabularia* (Bertl & Gradmann, 1987). The Characean K^+ channel shares several properties of its animal counterparts (Laver et al., 1989; Laver, Cherry & Walker, 1997), such as the large conductance (230 pS in cultured rat muscle; Barrett, Magleby & Pallotta, 1982; 200 pS in acinar cells of mouse lacrimal gland; Findlay, 1984) or open-closed distributions similar to those in the Ca^{2+}-activated K^+ channel in rat muscle (Magleby & Pallotta, 1983). The variation in Ca^{2+} sensitivity of individual channels in *Chara* is also similar to maxi-K channels of animal provenance (Moczydlowski & Latorre, 1983).

From a number of reports, data for cytoplasmic and vacuolar pH in *Characeae* are available that were obtained by different experimental approaches, but are consistent in their results. In general, *Characeae* maintain a cytosolic pH_{cyt} of about 7.8, responding with a decrease of about 0.4 pH units to the onset of darkness, whereas the vacuolar pH_{vac} was found to be in the range of 5–6.6 (Walker & Smith, 1975; Spanswick & Miller, 1977; Smith & Raven, 1979; Mimura & Kirino, 1984; Moriyasu, Shimmen & Tazawa, 1984*a;* Reid & Smith, 1988). It has been demonstrated that both cytosolic and vacuolar pH exerted a regulatory role on H^+ pumps in the tonoplast (Moriyasu, Shimmen & Tazawa, 1984*b;* Takeshige et al., 1988). Additionally, alkali cations affected their activities (Takeshige & Hager, 1988; Katsuhara et al., 1989). This is comparable to cation effects upon vacuolar H^+-pumps in higher plants, where H^+-ATPase and H^+-PPase are also colocalized (Rea & Poole, 1986; Hedrich et al., 1989). Experimental results obtained on higher plant vacuoles suggested that K^+ ions enhance PPase activity (Davies, Rea & Sanders, 1991) and, *vice versa,* the action of PPase may facilitate vacuolar K^+ accumulation (Davies, 1997).

A direct effect of H^+ upon conducting or gating properties of any ion channel has to be considered to be linked to the channel protein itself. All proteins contain acidic and basic side chains. Due to their ionizability those residues are important in determining the protein structure (Perutz, 1978) as well as its functional activity and stability (Matthew, 1985; Sharp & Honig, 1990; Raghavan, Lambright & Boxer, 1989; Yang & Honig, 1992, 1993; Yang & Barry, 1994).

Cook, Ikeuchi & Fujimoto (1984) had been the first to demonstrate that acidification of the cytoplasmic membrane face can inhibit maxi-K channel activation (pancreatic islet cells). Laurido et al. (1991) also showed that kinetics of the maxi-K channel (rat skeletal muscle) were affected by pH_{cyt}. Considering the present knowledge, it appeared reasonable to examine the *Chara* maxi-K channel with regard to its responsiveness to altered $[H^+]$: here, the immediate effect of H^+ on the electrical properties of the maxi-K channel is reported. Measurements were carried out on the membrane delineating cytoplasmic droplets prepared from *Chara australis* internodal cells. As previously reported (Lühring, 1986; Sakano & Tazawa, 1986), this membrane originates from the tonoplast of the intact cell.

Material and Methods

Plant Material

Chara australis was grown in plastic or glass containers at room temperature and at natural light/dark cycles. Internodal cells of 5 to 10 cm length were used for experiments. The procedures of preparation of cytoplasmic droplets had been previously described (Lühring, 1986). The sidedness of those droplets in most cases was right-side-out, i.e., the vacuolar face of the membrane was exposed to the bathing solution. An indication for this orientation was given by the observation that a few seconds after the droplet preparation, plastids that were enclosed began rotation and preserved it for hours. This is only possible when the cytosolic Ca^{2+} activity is reduced to less than 1 μM (Tominaga, Shimmen & Tazawa, 1983). Immobility of enclosed plastids under illumination strongly indicates that at least parts of the droplet membrane are inversely oriented.

Solutions

Cytoplasmic droplets were prepared in a solution containing (in mM): 150 KCl, 1 $CaCl_2$, 5 HEPES/Tris adjusted to pH 7.4. The same solution, but with varying pH, was used as the bathing medium in the experimental chamber and also as the filling solution of patch pipettes in inside-out experiments (the vacuolar side of the tonoplast faced the pipette interior). During excised-patch experiments, the patch was continuously superfused with test solution. In case of inside-out configuration, where the cytosolic membrane face was directed towards the perfusion system, the test solution did not contain additional Ca^{2+}, to prevent blockage of the maxi-K channel. Two buffer systems were used, one that contained sulfonic acids of different pK_a (Good buffers), the other one was composed of adequate amounts of KH_2PO_4 and K_2HPO_4 to give the desired final pH. Solutions employing Good buffers contained (in mM): 150 KCl, 5 MES (or PIPES, or HEPES, or CHES), adjusted to the desired pH. Solutions employing phosphate buffer contained (in mM): 140 KCl (adjusted to 150 K^+ by the buffer), 5–10 phosphate, adjusted to the desired pH. In case of outside-out experiments (the cytosolic membrane face was directed to the pipette interior), the pipette solution did not contain additional Ca^{2+}, whereas

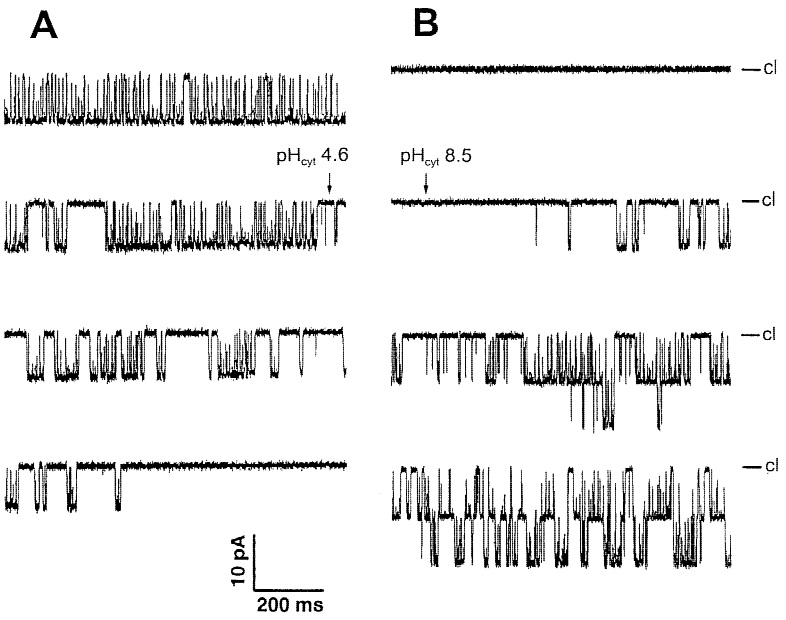

Fig. 1. Response of a single K^+ channel (maxi-K channel) in the tonoplast of *Chara australis* to cytosolic acidification. The test solutions contained (in mM): 140 KCl, 5–10 K_2H-/KH_2PO_4 (composed phosphate buffer to obtain the desired pH), final K^+ concentration was 150 mM. Pipette solution contained (in mM): 140 KCl, 1 $CaCl_2$, 6.5 K_2H-/KH_2PO_4 (10 mM K^+), pH 7. Corner frequency (8-pole Bessel low-pass): 2 kHz, clamp voltage: −40 mV. The perfusion system allowed for a solution exchange within 10 msec. The closed state is marked right-hand side in panel *B*. (*A*) Channel activity dramatically decreased upon lowering pH$_{cyt}$ from 8.5 to 4.6 (onset marked by downward arrow) at the cytoplasmic face of an excised inside-out patch. Within 2.7 sec activity gradually dropped to a completely closed state. (*B*) Upon changing pH$_{cyt}$ (downward arrow) from 4.6 to 8.5, the channel gradually resumed its former activity within 500 msec.

the test solutions were composed as mentioned above but additionally contained 1 mM $CaCl_2$.

Electrophysiology

Inside-out and outside-out measurements (Hamill et al., 1981) were carried out on the tonoplast. The nomenclature that applies to intact cells is also used for the droplet membrane: the cytosolic compartment (inside) is enclosed by a naturally oriented membrane, and the vacuolar compartment (outside) is simulated by the bathing solution. Patch pipettes were drawn from borosilicate hard-glass (Hilgenberg, Malsfeld Germany, type 11032) to open diameters of less than 1 μm (determined by scanning electron microscopy), giving an electrical resistance of about 20 MΩ in 150 mM KCl.

Single channel currents were recorded by a commercial current-to-voltage converter (Axopatch 200A, Axon Instruments, Foster City, CA), digitized (VR-10, Instrutech, NY) and stored on videotape. For off-line analysis, the played-back signals were conditioned by an 8-pole Bessel low-pass filter (mod. 816, Rockland, NJ) and the output fed into a computer. Analysis was performed with pCLAMP software (Axon Instruments). The kinetic model of the gating reaction was chosen according to Laver and Walker (1987). A serial 5-state model turned out to match the measured time-series almost perfectly compared to alternative models, where systematic errors in validating plots of open and closed times distributions occurred. Rate constants were also analyzable in multichannel recordings by implementation of an algorithm treating the activity of several uniform channels as that of a single macrochannel. From the measured time series the noise-free gating sequence of the channel was reconstructed by means of a 4th order Hinkley detector (Hinkley, 1970; Schultze & Draber, 1993). The level for detection was automatically adjusted to the noise level in order to give only one false alarm per 105 samples. The analyzing program had a book-keeping algorithm which constructed the dwell-time histograms from the reconstructed time series. These dwell-time histograms were subjected to a multichannel target fit, i.e., the rate constants of the selected Markov model were adjusted under the guidance of a simplex algorithm (Press et al., 1987) until good fits of the multichannel dwell-time histograms were obtained (Blunck et al., 1998). Data were digitized with a sampling rate of 20 kHz, after conditioning raw data with an anti-aliasing filter set to 8 kHz corner frequency. Analysis and fitting of the data were achieved by utilizing the target fit program 'Day', designed by the group of U.P. Hansen (Institute of Applied Physics, University of Kiel, Germany). Although subconductant states had previously been demonstrated (Lühring, 1986; Tyerman, Terry & Findlay, 1992) and had been taken into account by Laver et al. (1997) in analyzing gating kinetics of this channel, a substate-sensitive analysis was not applied in this study because the appearance of a subconductant state was only rarely observed (a few among thousands of events).

Results

In excised patches, the inside-out-oriented K^+ channel is blocked by cytosolic Ca^{2+} ($EC_{50} \geqslant 100$ μM) such that both, inward and outward currents, are suppressed. Therefore, in the course of inside-out experiments, test solutions were applied that did not contain Ca^{2+} in excess of those levels arising from salt contaminations (1 μM range). The K^+ concentration of 150 mM was chosen, because a previous investigation revealed that the channel conductance is tending to saturate at K^+ concentrations beyond 132 mM (Lühring, 1986). At concentrations as high as 300 mM the single channel conductance is even greater, however possible modification of the channel protein by high ionic strength should be avoided. Under these conditions, the observed single channels could retain their active or activatable states as well as their conductance during superfusion for more than 30 minutes.

Figure 1 shows representative traces of current fluctuations recorded from a single maxi-K channel at varying cytosolic pH (pH$_{cyt}$). Clearly, the channel that dis-

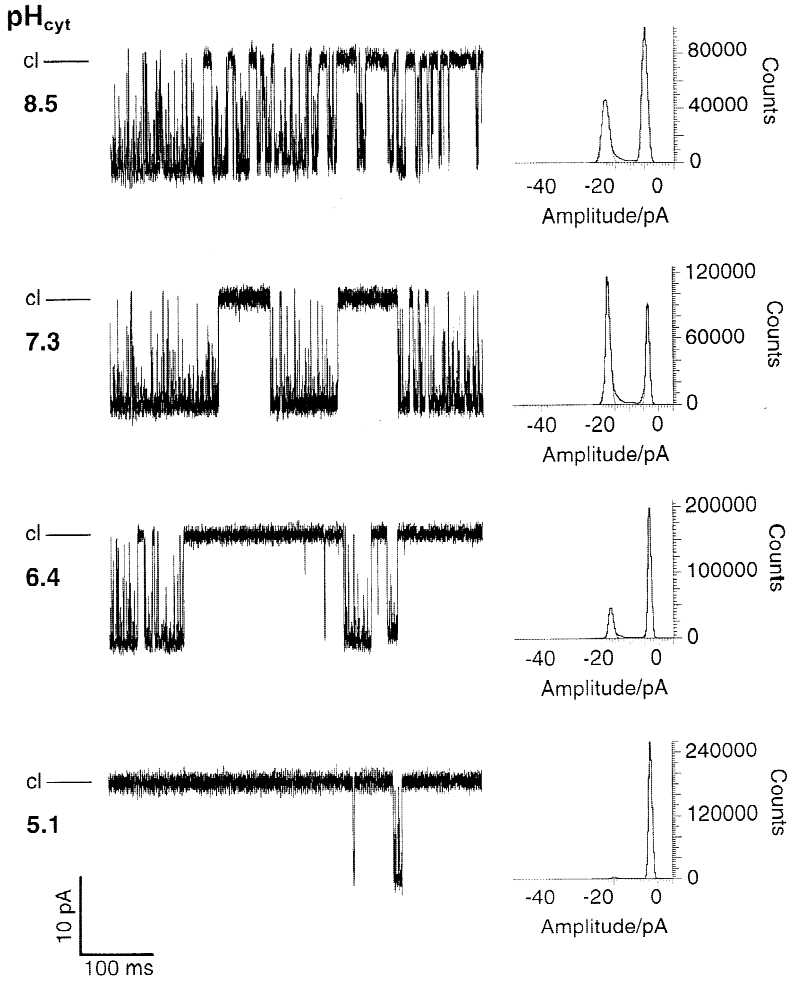

Fig. 2. Effect of pH_{cyt} on gating of the maxi-K channel in the tonoplast of *Chara australis.* An excised patch from the membrane delineating a cytoplasmic droplet that contained a single K^+ channel was superfused in an inside-out configuration with solutions of different pH_{cyt}. Left-hand side, current traces of 512 msec duration each are displayed, where closed levels are marked by left-hand side and the actual pH_{cyt} is given beneath. Right-hand side, the corresponding all-point amplitude histograms are shown that were constructed from record intervals of 51 sec. With only small deviations at the conditions applied here, channel conductance amounted to 165 ± 6 pS, whereas the open probability decreased distinguishedly with decreasing pH_{cyt} (39.5% at pH_{cyt} 8.5, 61.3% at pH_{cyt} 7.3, 26% at pH_{cyt} 6.4, 2.2% at pH_{cyt} 5.1). Test solutions contained (in mM): 150 KCl, 5 CHES (or HEPES pH 7.3, PIPES pH 6.4, MES pH 5.1, respectively). Corner frequency (8-pole Bessel low-pass): 5 kHz, clamp voltage: −80 mV. Pipette solution contained (in mM): 150 KCl, 1 $CaCl_2$, 5 HEPES/Tris, pH 7.4.

played bursting behavior was markedly affected by acidification of the cytoplasm-sided solution. While its conductance remained almost unchanged, the gating mechanism of the channel obviously was the target for H^+. Upon exchanging the medium of pH_{cyt} 8.5 for an identical solution of pH_{cyt} 4.6, channel activity gradually decreased to an eventually permanent closed state (panel *A* of Fig. 1). The pH_{cyt}-induced inactivation was reversed by superfusing the medium of pH_{cyt} 8.5 (panel *B* of Fig. 1). Figure 2 representatively shows current fluctuations through the maxi-K channel at different pH_{cyt}. Amplitude histograms that were constructed from this recording over an interval of 51 sec are displayed right-hand side of the respective current traces. In those amplitude histograms, the total recording time is represented by the area covered by the two fitted Gaussian distributions above the conductance states (open and closed). Open probabilities are given by the ratio of the time the channel spent in the open state (open peak area) over the total recording time. The open probabilities (P_o) of the K^+ channel exhibit a strong dependency on cytosolic pH_{cyt}. P_o significantly decreased with decreasing pH_{cyt}. At pH_{cyt} 8.5, the channel bursted with highest frequency, however, the open state was more short-lived. Figure 3*A* shows that with increasing hyperpolarization of the tonoplast at pH_{cyt} 7.0, P_o increased due to an increase in burst frequency. At pH_{cyt} 5.9 (Fig. 3*B*), this voltage-dependent P_o increase was preserved, however, burst durations were shorter and extraburst intervals significantly greater than at neutral or slightly alkaline pH_{cyt} at the respective clamp voltage.

Figure 4 displays current responses upon applied voltage ramps from −100 to +100 mV (50 msec interval) of a single K^+ channel recorded on an inside-out patch during superfusion with test solutions of different pH_{cyt}. The resulting *IV* curves demonstrate that the channel conductance is largely independent of pH_{cyt} changes (189 pS at pH_{cyt} 8.5, 183.5 pS at pH_{cyt} 7.7, 168 pS at pH_{cyt} 7.0, 172.3 pS at pH_{cyt} 6.6, 163.5 pS at pH_{cyt} 5.9). Although a maximal difference of about 20 pS can be stated in these measurements, the major effect of decreased pH_{cyt} has to be seen in the altered kinetics of transitions between open and closed states. Note the absence of outward-current attenuation (*cf.,* Fig. 5). A

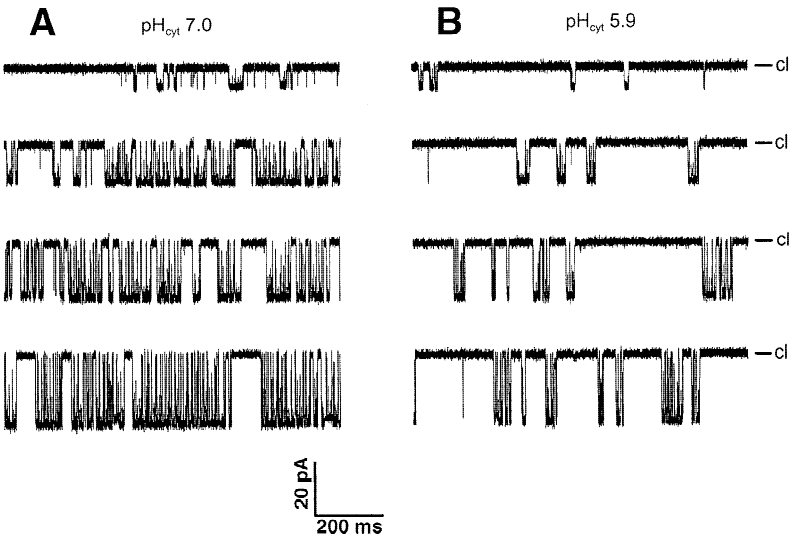

Fig. 3. Effects of pH_{cyt} and voltage on gating of the maxi-K channel in *Chara* tonoplast. The number of transitions is increasing with increasing voltage (from top to bottom −40, −80, −120, and −160 mV in both panels). Extraburst closed times and burst durations, as well, are markedly depending on pH_{cyt} (*A* pH_{cyt} 7.0, *B* pH_{cyt} 5.9). The closed level is indicated right-hand side at each trace. Inside-out configuration. Test solutions contained (in mM): 140 KCl, 6.5 or 9.1 K_2H-/KH_2PO_4 (10 mM K^+), pH 7 or 5.9, respectively. Pipette solution (in mM): 140 KCl, 1 $CaCl_2$, 6.5 K_2H-/KH_2PO_4 (10 mM K^+), pH 7. Corner frequency (8-pole Bessel low-pass): 5 kHz.

similar recording on an outside-out patch, i.e., where the vacuolar face of the tonoplast had been exposed to solutions of different pH (pH_{vac}), is shown in Fig. 5. Similar to *IV* curves obtained from inside-out patches, the K^+ conductance determined from the slope of the inward current was not affected by varying pH_{vac}. The channel conductance at all conditions was 163.5 pS, except that at pH_{vac} 7.3, where conductance slightly increased to 167.8 pS. In these experiments, attenuation of outward current was observed which approached a saturation level of about 10 pA in a voltage range of 75–100 mV, whereas no inward saturation became evident over the applied negative voltage range. It may be assumed, however, that saturation under these experimental conditions will occur at membrane voltages exceeding −150 mV, as reported previously (Lühring, 1986).

Inhibition kinetics of H^+ are displayed in Fig. 6. Decreasing pH_{cyt} at the cytosolic channel face reduced the relative open probability of the maxi-K channel. Fitting the data with the Hill equation revealed a pK_a of 6.56, and a slope of 2.05, indicating a cooperative protonation process of at least two cytoplasm-accessible target sites. This Hill plot is the result of a data compilation from different experiments on long-lived patches containing a single channel each. Within each experimental series, P_o values at either pH_{cyt} were related to the pH_{cyt}-dependent maximum ($P_{o,max}$) observed. The advantage of using relative P_o values is that data obtained at various membrane voltages can be employed correspondingly.

Inhibition kinetics by varying pH_{vac} could not be analyzed by a Hill plot similar to that shown for pH_{cyt} because more than one component of the gating reaction is altered by acidification of the extraplasmatic solution. At low pH_{vac}, tail currents in macroscopic current recordings decayed by exhibiting at least two kinetic components, a rapid voltage-dependent current decrease, and a slow resumption of outward current following the fast inactivation (*data not shown*).

Steady-state open probabilities are shown in Fig. 7. These curves had emerged from patches containing single channels that were recorded for 2–3 minutes at either clamped voltages. At high pH applied to both sides of the membrane, a peak open probability is found at −120 to −150 mV, whereas low pH_{vac} shifted the voltage sensitivity towards depolarized voltage with a maximum at around −40 mV. Low pH_{cyt} did not cause such a dramatic shift. The Boltzmann distribution of voltage-dependent open probabilities divulged the effect of pH on the maxi-K channel (Fig. 8). From these distributions it can be seen that a decrease in pH_{cyt} and pH_{vac} indeed reduced open probabilities towards zero, while pH_{vac} shifted voltage sensitivity of the channel more than pH_{cyt} (voltages of half-maximal activation were determined as $V_{1/2} = -83$ mV at pH_{cyt} 7.0, $V_{1/2} = -63$ mV at pH_{cyt} 5.9, $V_{1/2} = -102$ mV at pH_{vac} 7.3, and $V_{1/2} = +5$ mV at pH_{vac} 5.1). The slope of those curves (representing the apparent gating charge) were determined to be 2.6 at pH_{cyt} 7, and 1.3–1.4 at pH_{cyt} 5.9, pH_{vac} 7.3, and pH_{vac} 5.1, respectively. The sensitivity to 10-fold H^+ concentration changes ($\Delta pH_{cyt,vac}$) was 18 mV/ΔpH_{cyt} and 42 mV/ΔpH_{vac}, respectively.

The noticeable effect of H^+ upon kinetics of the K^+ channel challenged an attempt to examine transition rates in a presumptive gating reaction scheme for their possible response to H^+. A 5-state gating model was applied to the maxi-K channel, of the form

$$C_1 \underset{k_{21}}{\overset{k_{12}}{\rightleftharpoons}} C_2 \underset{k_{32}}{\overset{k_{23}}{\rightleftharpoons}} C_3 \underset{k_{\alpha 3}}{\overset{k_{3\alpha}}{\rightleftharpoons}} O_\alpha \underset{k_{\beta\alpha}}{\overset{k_{\alpha\beta}}{\rightleftharpoons}} O_\beta \qquad \text{(Scheme I)}$$

Five states must be postulated as the minimum, be-

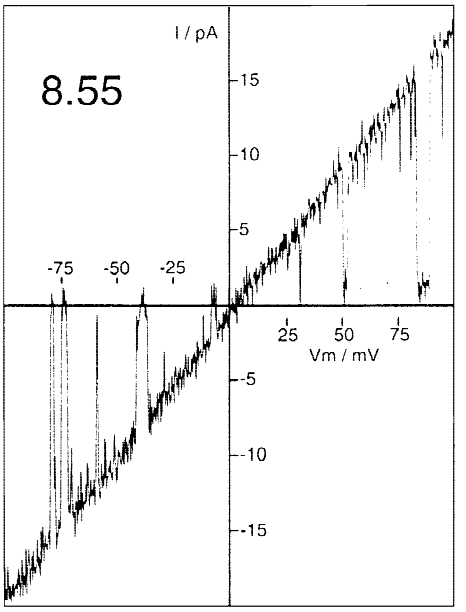
I / pA
8.55
15
10
5
-75
-50
-25
25
50
75
Vm / mV
-5
-10
-15

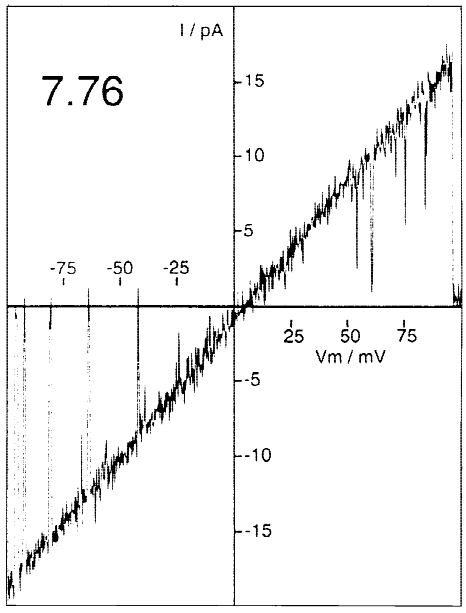
I / pA
7.76
15
10
5
-75
-50
-25
25
50
75
Vm / mV
-5
-10
-15

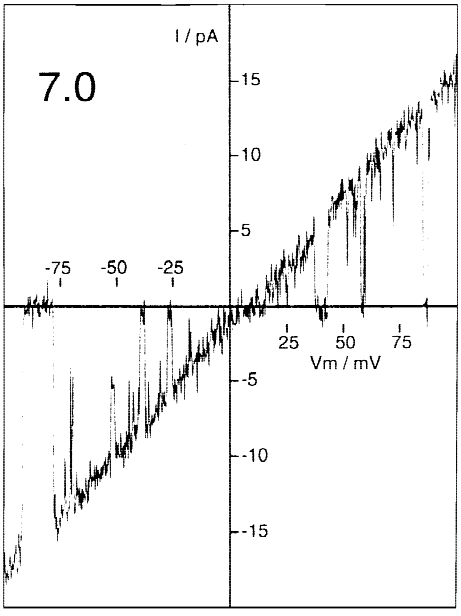
I / pA
7.0
15
10
5
-75
-50
-25
25
50
75
Vm / mV
-5
-10
-15

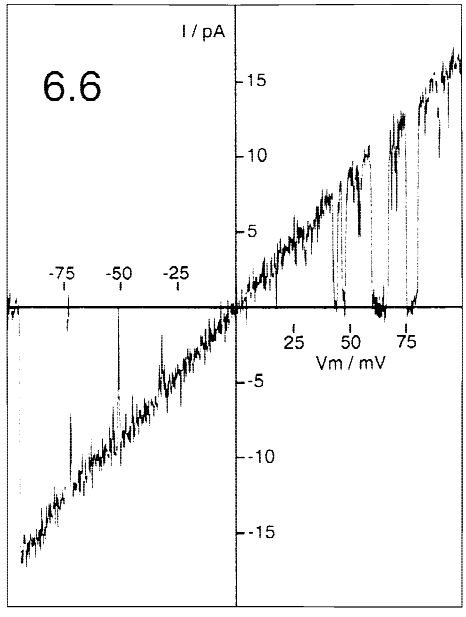
I / pA
6.6
15
10
5
-75
-50
-25
25
50
75
Vm / mV
-5
-10
-15

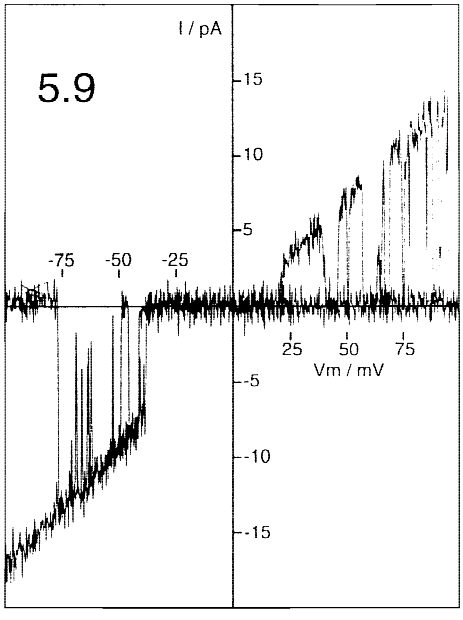
I / pA
5.9
15
10
5
-75
-50
-25
25
50
75
Vm / mV
-5
-10
-15

Fig. 4. Effect of pH_{cyt} on current response upon voltage ramps from −100 to +100 mV (50 msec period) of the maxi-K channel. An excised patch in inside-out configuration that contained a single K^+ channel was superfused with test solutions of different pH_{cyt}. During superfusion, current was recorded while the voltage ramp was driven. At each condition, two voltage clamp runs were recorded, one without channel activity, the other one with the channel displaying current fluctuations. The blank was subtracted from the recording with the active channel which resulted in an *IV* curve of the open channel. At pH_{cyt} 5.9, two runs are displayed because the channel exhibited activity only either at negative or positive voltages during several runs. The actual pH_{cyt} of either solution is given in the corresponding panel. Test solutions contained (in mM): 140 KCl, 5–10 K_2H-/KH_2PO_4 (composed to yield the final pH). Phosphate buffer concentration was corrected to obtain a final K^+ concentration of 150 mM, phosphate concentration varied between 5 and 10 mM. Pipette solution contained (in mM): 150 KCl, 1 $CaCl_2$, 5 HEPES pH 7.3. Corner frequency (8-pole Bessel low-pass): 5 kHz.

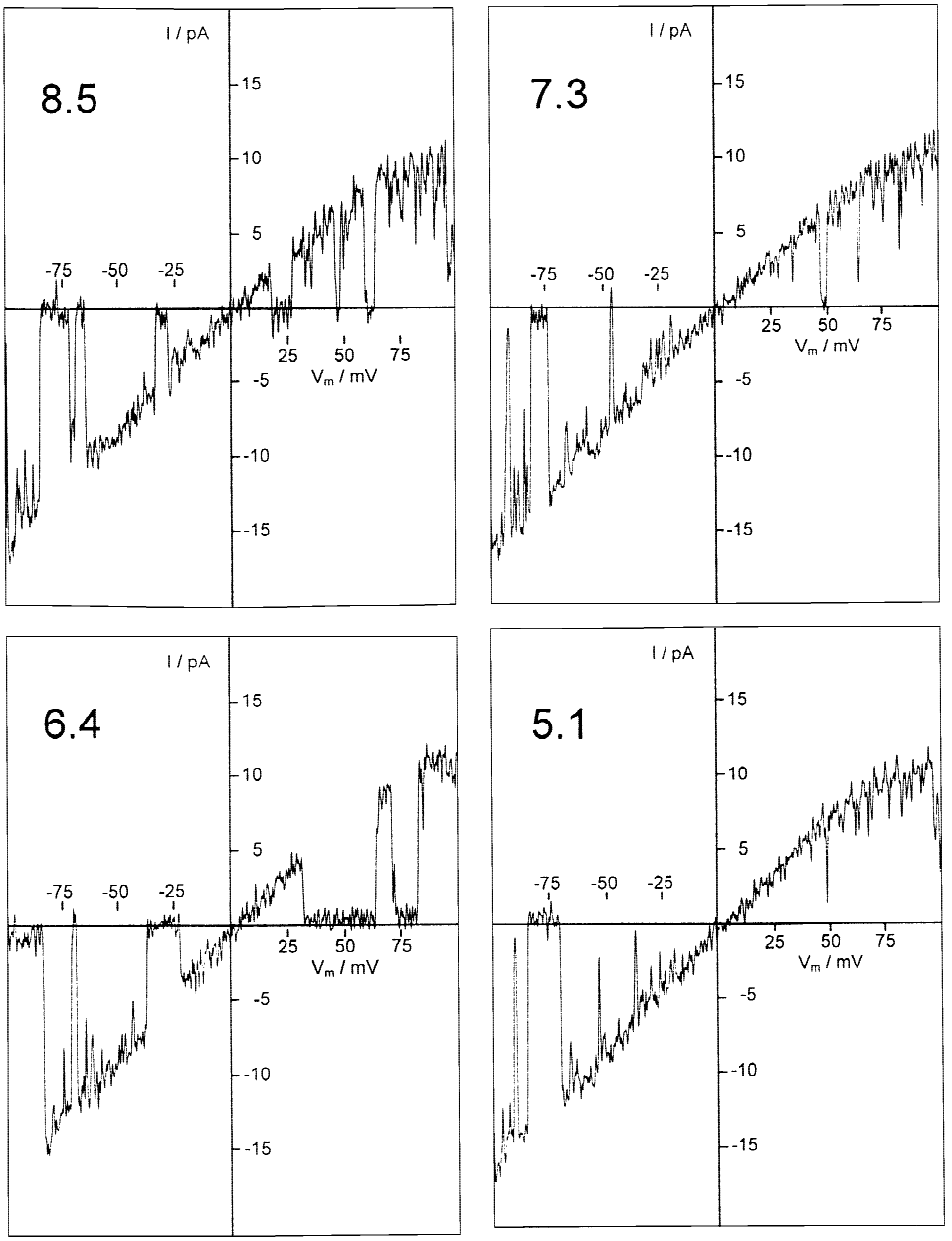

Fig. 5. Effect of pH_{vac} on current response upon voltage ramps from −100 to +100 mV (50 msec period) of the maxi-K channel. An excised patch in outside-out configuration containing a single K^+ channel was superfused with test solutions of different pH_{vac}. *IV* curves were obtained as explained in Fig. 4. pH_{vac} is given in each panel. Test solutions contained (in mM): 150 KCl, 1 $CaCl_2$, 5 CHES pH 8.5 (or HEPES pH 7.3, PIPES pH 6.4, MES pH 5.1). Pipette solution contained (in mM): 150 KCl, 5 HEPES pH 7.3. Corner frequency (8-pole Bessel low-pass): 5 kHz.

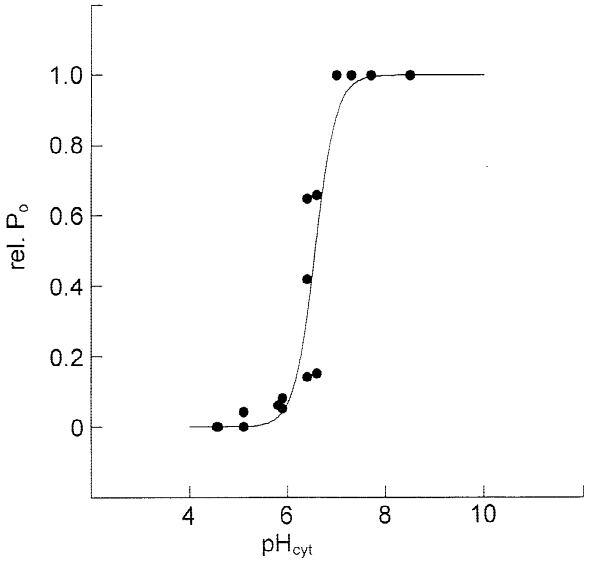

Fig. 6. pH_{cyt}-dependent inhibition kinetics of the maxi-K channel. Relative open probabilities (evaluated as described in Results) determined from a multitude of single channel recordings at different pH_{cyt} were plotted versus pH_{cyt}. Data points were fitted by a Hill equation of the form rel.$P_o = [H^+]^n \cdot (K_a^{*n} + [H^+]^n)^{-1}$ (solid line), where n is the number of binding sites, and K_a^* the apparent dissociation constant that comprises factors of interaction and the intrinsic dissociation constant. A pK_a^* of 6.56 and a Hill coefficient of $n = 2.05$ characterize the kinetics.

cause less than three closed states or less than two open states resulted in systematic errors in fitting the frequency distributions either of the open or the closed dwell times with sums of a respective number of exponential functions (*see*, Fig. 9). However, extremely prolonged closed times were also observed. Due to time-limited recording intervals, those events did not contribute significantly to dwell-time fits. Although this long-lived closed state should be included into the scheme, it was not considered in the evaluation of rate constants, because dwell-time distributions were satisfactorily fitted with three exponential terms. In a previous report (Laver & Walker, 1987), a gating model for this K^+ channel was proposed that comprised at least 7 closed states and 1 open state in a series grouping. Those authors suggested a voltage-dependent gating reaction, where the open state is engirded at both ends by closed states. One group of these closed states (termed A_1 through A_4 in that report) becomes predominant at negative voltages, whereas, at positive voltages the other group (B_1 to B_3) determines closed life times (*cf.*, Scheme 3 in the above cited report). In their analysis, they omitted the second open state (O_β) due to lack of data. During evaluation of transition rates, I encountered a distinguished individuality in kinetic behavior of the single maxi-K channel, evidenced by the wide range of absolute rate constants, occurring even in the same patch under constant experimental conditions. These variations were already known before (Laver & Walker, 1987). For $V_m = -40$ mV at pH_{vac} 7.3 and 5.1, respectively, absolute rate constants are given in Table 1. These experimental conditions were chosen with regard to in vivo physiological conditions: K^+ concentrations in the cytoplasm and the vacuole had been determined to be about 70 and 110 mM, respectively (Reeves, Shimmen & Tazawa, 1985; Okihara & Kiyosawa, 1988) vacuolar sap is of about pH 5 (*cf.*, Introduction), voltage across the tonoplast is −10 to −40 mV in *Characeae* (cytoplasm negative, Findlay & Hope, 1964; Hayama, Nakagawa & Tazawa, 1979; Shimmen & Nishikawa, 1988). The data presented here were evaluated by a target fit of dwell-time distributions to the presumptive 5-state model. The probabilities of occupancies of either state are given in Table 2. Those probabilities were calculated from absolute rate constants, given in Table 1, according to the following equations:

$$P_{C_1} = \left\langle 1 + \frac{k_{12}}{k_{21}} \cdot \left\{ 1 + \frac{k_{23}}{k_{32}} \cdot \left[1 + \frac{k_{3\alpha}}{k_{\alpha 3}} \cdot \left(1 + \frac{k_{\alpha\beta}}{k_{\beta\alpha}} \right) \right] \right\} \right\rangle^{-1}, \quad (1)$$

$$P_{C_2} = \left\{ 1 + \frac{k_{21}}{k_{12}} + \frac{k_{23}}{k_{32}} \cdot \left[1 + \frac{k_{3\alpha}}{k_{\alpha 3}} \cdot \left(1 + \frac{k_{\alpha\beta}}{k_{\beta\alpha}} \right) \right] \right\}^{-1}, \quad (2)$$

$$P_{C_3} = \left[1 + \frac{k_{32}}{k_{23}} \cdot \left(1 + \frac{k_{21}}{k_{12}} \right) + \frac{k_{3\alpha}}{k_{\alpha 3}} \cdot \left(1 + \frac{k_{\alpha\beta}}{k_{\beta\alpha}} \right) \right]^{-1}, \quad (3)$$

$$P_{O_\alpha} = \left\{ 1 + \frac{k_{\alpha\beta}}{k_{\beta\alpha}} + \frac{k_{\alpha 3}}{k_{3\alpha}} \cdot \left[1 + \frac{k_{32}}{k_{23}} \cdot \left(1 + \frac{k_{21}}{k_{12}} \right) \right] \right\}^{-1}, \quad (4)$$

$$P_{O_\beta} = \left\langle 1 + \frac{k_{\beta\alpha}}{k_{\alpha\beta}} \cdot \left\{ 1 + \frac{k_{\alpha 3}}{k_{3\alpha}} \cdot \left[1 + \frac{k_{32}}{k_{23}} \cdot \left(1 + \frac{k_{21}}{k_{12}} \right) \right] \right\} \right\rangle^{-1}. \quad (5)$$

Rate constants compare well with those determined by Laver and Walker (1987). Occupancy probabilities of the states are in agreement with the open probabilities in Fig. 7 (*cf.*, data at −40 mV). At pH_{vac} 7.3, the sum of P_{O_α} + P_{O_β} is 14%, whereas it is 6.3% at pH_{vac} 5.1. Clearly, a major effect of low pH_{vac} is the 18.7% increase of dwelling in state C_1 (*see*, Table 2).

Probabilities that a state will be abandoned in a forward or backward direction, respectively, were plotted *vs.* voltage (e.g., the probability to leave the closed state C_2 in a forward direction towards the open state is given by $P_{23} = k_{23} \cdot (k_{21} + k_{23})^{-1}$). These probabilities show an acceptable consistency between recordings also on different patches. Figure 10 displays those probabilities of forward reactions, at two different pH_{vac} applied to excised outside-out patches (the respective backward

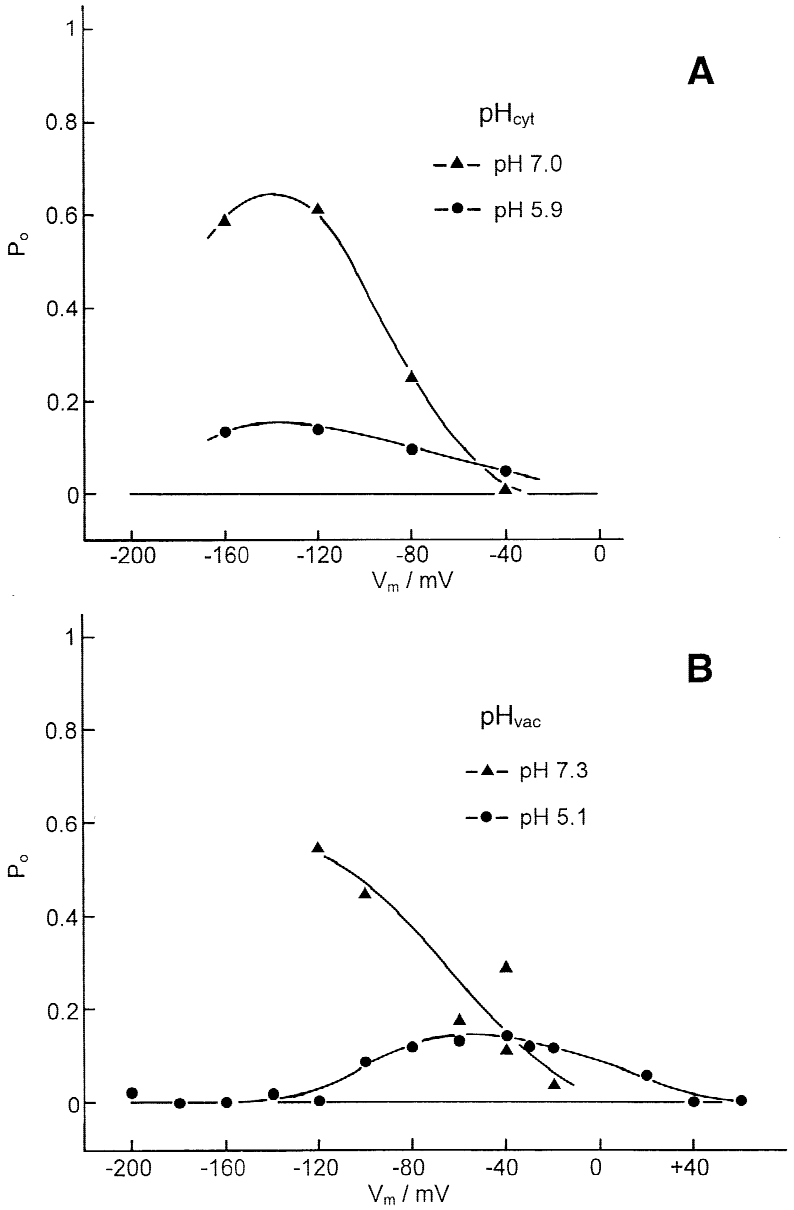

Fig. 7. K^+ channel open probabilities as a function of membrane voltage at different pH. (*A*) At cytosolic pH 7, open probability reached a maximum value of about 60% at −120 mV and decreased to almost zero when the membrane was depolarized. At pH 5.1, open probability was suppressed to about 10%, whereas its maximum was retained at −120 mV. (*B*) At pH_{vac} 7.3, the open probability showed approximately identical characteristics, however, after lowering pH_{vac} to 5.1, the maximum of open probability of about 10% was shifted to a more positive value at −50 mV.

transition probabilities are reflections of those data at the 50% line, i.e., at $P_{ij} = 0.5$, as the axis of symmetry). Panel *A* of Fig. 10 shows that at pH_{vac} 7.3 the channel protein will leave its closed state C_2 preferably in open state direction (P_{23}) at voltages more negative than −40 mV (70–80%), but with a higher probability falls back into state C_1 at depolarized voltages. The probability for a transition from the closed state adjacent to open ($P_{3\alpha}$) is less pronounced (about 60%) and also decreases with proceeding depolarization. A similar behavior is shown for the transition probability from open state O_α to O_β ($P_{\alpha\beta}$, about 60% down to −40 mV). At pH_{vac} 5.1 (Fig. 10*B*), those probabilities had changed markedly. From closed state C_2, the channel preferably dropped back into state C_1 (P_{21}, 80%) at far negative voltages, but assumes a high forward preference at about −50 mV (P_{23}, 80%), rapidly decreasing with proceeding depolarization and reaches a minimum at positive voltages. The forward reaction out of closed state C_3 ($P_{3\alpha}$) displays a similar behavior at negative voltages, but maintains a high forward probability also at positive voltages. The transition probability out of open state O_α towards O_β ($P_{\alpha\beta}$) is similar to that shown in panel *A* at pH_{vac} 7.3.

Discussion

The highly conductant K^+ channel in the tonoplast of Characean internodal cells is similar in its behavior to animal maxi-K channels (Barrett et al., 1982; Marty,

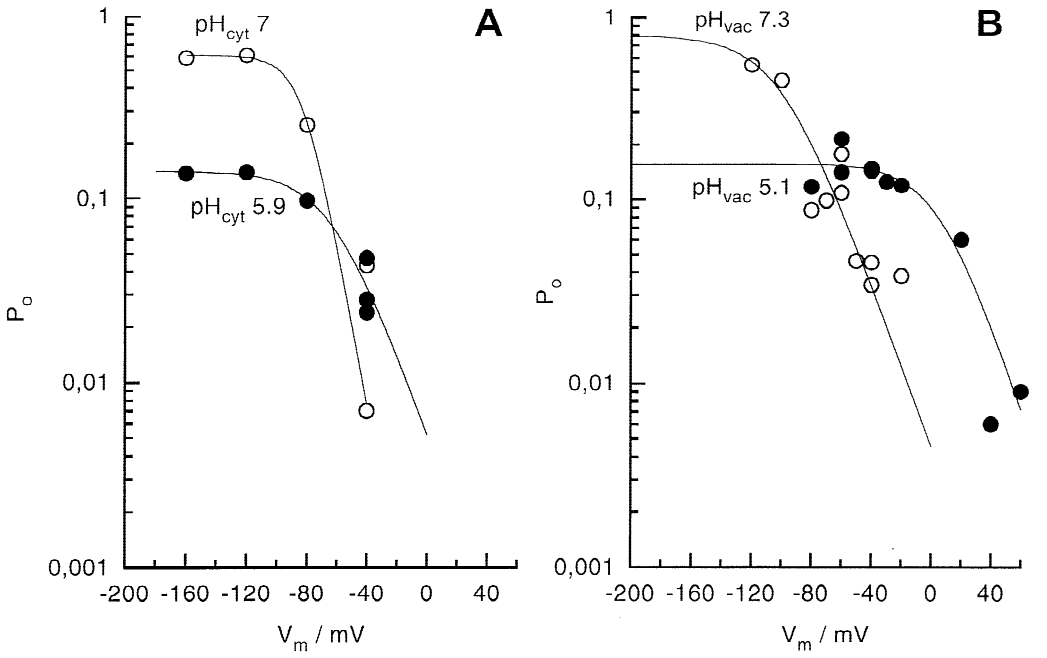

Fig. 8. Effect of pH_{cyt} (*A*) and pH_{vac} (*B*) on Boltzmann distribution of the K^+ channel. Open probabilities are plotted *vs.* membrane voltage. Data were fitted with the Boltzmann equation $P_o = P_{o,max} \cdot \{1 + \exp[(V_m - V_{1/2}) \cdot z \cdot \varepsilon/(kT)]\}^{-1}$ (solid line) where $V_{1/2}$ denotes the voltage of half-maximal activation, z the apparent gating charge, and ε the elementary charge, k and T are the Boltzmann constant and the absolute temperature, respectively. Only acidification of the vacuolar side of the channel led to a shift of activation characteristics.

1983; Latorre & Miller, 1983; Bell & Miller, 1984; Yellen, 1984; Eisenman, Latorre & Miller, 1986; Blatz & Magleby, 1987; Cecchi et al., 1987; Butler et al., 1993) with respect to conductance, selectivity and kinetics, except that it is inward rectifying (Laver et al., 1989). This algal maxi-K channel exhibits a marked responsiveness to changes in cytosolic and vacuolar pH (pH_{cyt}, pH_{vac}). Decreasing pH_{cyt} from a slightly alkaline level leads to a gradual decrease in its open probability (P_o), whereas channel conductance is hardly affected (Figs. 1 and 2). At pH_{cyt} 5 the K^+ channel is almost completely inactive, however, this effect is reversible (Fig. 1). Basically, the voltage dependency of P_o is preserved at low pH_{cyt}, indicated by an increase in burst frequency with increasing negative voltage (Fig. 3). Current-voltage relationships recorded for changes in both, pH_{cyt} and pH_{vac}, (Figs. 4, 5), respectively, show the continuity of channel conductance over the whole pH range. This indicates that H^+ ions, even if they traverse the channel, do not significantly change pore conductance.

A phenomenon becomes visible by comparing the *IV* curves recorded at different patch configurations. While the outside-out-oriented channel shows current saturation at positive voltage, the outward current through the inside-out-oriented channel develops linearly with increasing voltage. Since this was observable only during inside-out configuration and superfusion of the patch with test solutions, it might be interpreted as a wash-off effect of some cytosolic component contributing to the saturation characteristics. No experiments have been carried out to date to examine this hypothesis.

pH_{cyt}-sensitive open probabilities of the single maxi-K channel could be fitted with the Hill equation (Fig. 6). The slope of $n = 2.05$ suggests that at least 2 H^+ binding sites exist in the cytosolic pore region. The pK_a 6.56 could be compatible with the supposition that histidine residues might be responsible. Similar results ($pK_a \approx 6.8$) were obtained on the slowly activating vacuolar channel from *Vicia faba* tonoplast (Schulz-Lessdorf & Hedrich, 1995) except that those authors did not observe cooperativity ($n = 0.76$). Possibly, the Ca^{2+} binding site existing at the cytoplasm-sided pore region (Laver, 1990) is also responsible for H^+ binding. This was suggested for animal maxi-K channels previously (Cook et al., 1984; Christensen & Zeuthen, 1987; Kume et al., 1990) but contradicted by Laurido et al. (1991) who concluded that H^+ does not compete with Ca^{2+} at Ca^{2+}-binding sites, rather H^+ should weaken Ca^{2+} binding to all conformational states, furthermore that proton sites are located outside the ion conduction system. Kinetic models of competitive or noncompetitive interaction of H^+ and Ca^{2+} binding sites have not been considered in the present work.

The gating scheme used in this work can be made compatible with that proposed by Laver and Walker (1987). By application of negative clamp voltages, the closed states $C_{1,2,3}$ correspond to states $A_{1,2,3,4}$ of those authors, except that, here, C_1 comprises both, A_1 and A_2.

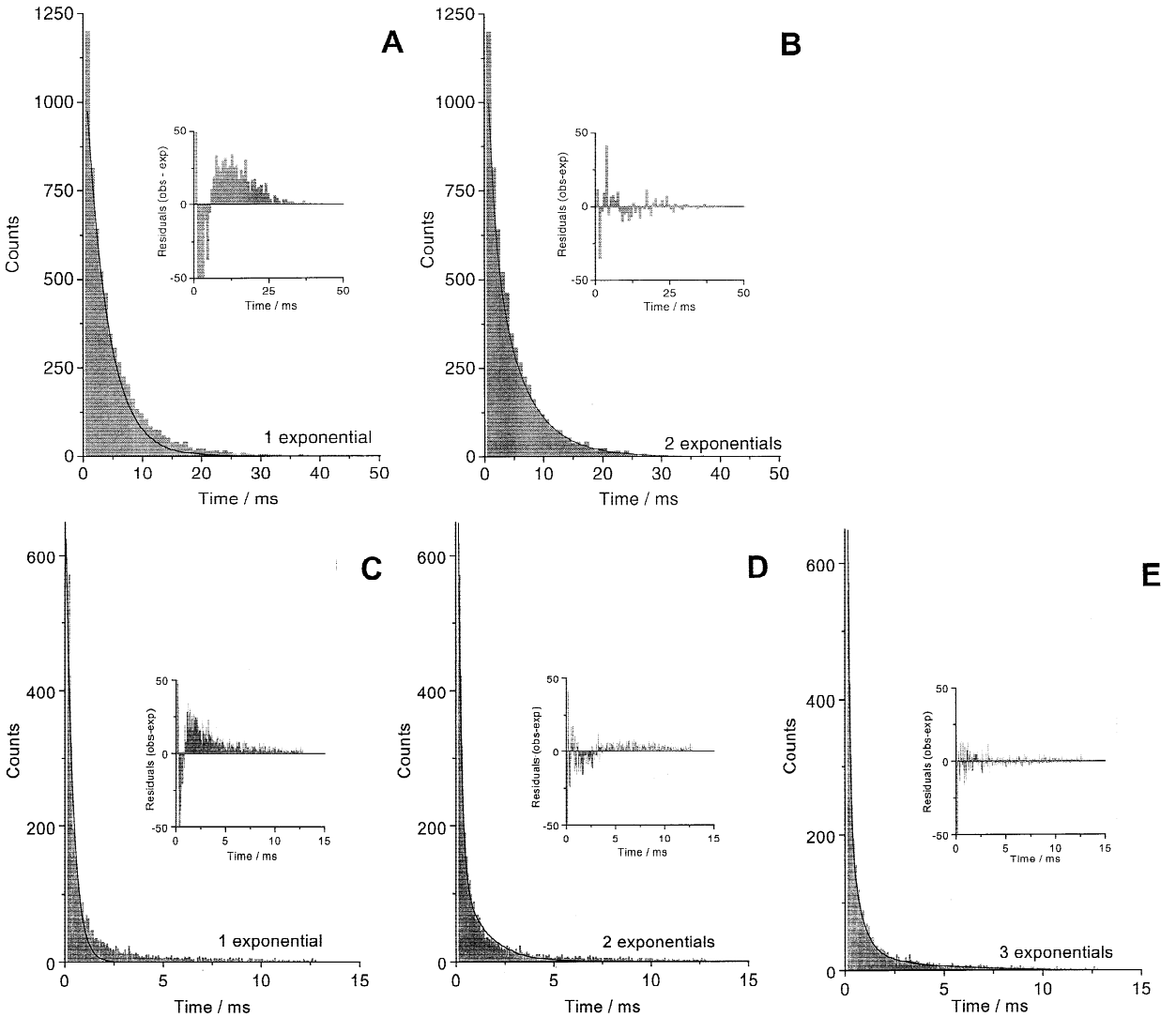

Fig. 9. Dwell-time distributions of the maxi-K channel fitted with a varying number of exponential terms. Inside-out configured excised patch superfused with (in mM): 150 KCl, 5 HEPES, pH 7.3; pipette solution (in mM): 150 KCl, 1 $CaCl_2$, 5 HEPES, pH 7.3. Recording interval: 61 s, sampling rate: 20 kHz, low-pass filter: 5 kHz. Decay of open (panels *A*, *B*) and closed (*C–E*) dwell-time distributions. Distributions were fitted with sums of exponential terms of the form $f(t) = \sum_i A_i \cdot \tau_i^{-1} \cdot \exp(-t/\tau_i)$. The decline of residuals (as the difference between observed and expected values), shown as insets in the respective diagrams, infer that two and at least three exponential terms are required to fit the open and closed dwell-time distributions, respectively. Employing less exponential terms led to systematic errors seen in the residuals (for open decay, see panel *A*, for closed decay, see panels *C* and *D*).

At positive voltages, $C_{1,2,3}$ can be considered to represent their closed states group $B_{1,2,3}$.

The major determinant of the mean life-time of the open channel has to be assigned to the transition probabilities between C_3 and $O_{\alpha,\beta}$, where C_3 represents the short closed intervals during a burst. Thus, both C_3 and $O_{\alpha,\beta}$ belong to the burst event. The duration of the burst should then be depending on the backward transition rate from C_3 to C_2, and *vice versa*, the burst frequency be determined by the forward rate C_2 to C_3. Those transition probabilities into ($C_2 \rightarrow C_3$) and out of the burst state ($C_3 \rightarrow C_2$), respectively, are reflected in Fig. 10. The voltage-dependent forward reaction from C_2 into the burst states is favoured at pH_{vac} 7.3, but suppressed at physiological pH_{vac} 5.1. The pH_{vac}-induced shift of the position of the bell-shaped curve describing voltage dependency of P_o (*cf.*, Laver & Walker, 1987) might be caused by the increased transition probability into the open state at depolarized voltage. A simultaneous reduction in open probability at negative voltage should be due to the inability of the channel to enter the burst level.

The absolute rate constants obtained in these experiments (Table 1) are in agreement with those published by Laver & Walker (1987, Table 2 therein). The probabili-

Table 1. Rate constants of transitions (given in sec^{-1}) between kinetic states of the *Chara* maxi-K channel obtained by fitting of dwell-time histograms (Blunck et al., 1998)

	Forward reaction		Backward reaction		Uncertainty
pH_{vac} 7.3	k_{12}:	10	k_{21}:	75	30–60%
	k_{23}:	550	k_{32}:	1750	50%
	$k_{3\alpha}$:	2350	$k_{\alpha 3}$:	1150	30–50%
	$k_{\alpha\beta}$:	2200	$k_{\beta\alpha}$:	1800	30–50%
pH_{vac} 5.1	k_{12}:	10	k_{21}:	700	70–100%
	k_{23}:	500	k_{32}:	1300	30–75%
	$k_{3\alpha}$:	3100	$k_{\alpha 3}$:	850	25–40%
	$k_{\alpha\beta}$:	1700	$k_{\beta\alpha}$:	700	25–50%

Subscripts indicate the direction of transitions according to the gating model depicted in the text (for k_{ij}, e.g., $C_i \xrightarrow{k_{ij}} C_j$). Mean values from 5 experiments presented for $V_m = -40$ mV.

Table 2. Probabilities of occupancies (P) in the 5-state model at $V_m = -40$ mV

P_i	% of Occupancy	
	pH_{vac} 7.3	pH_{vac} 5.1
P_{C_1}	73.2	91.9
P_{C_2}	9.8	1.3
P_{C_3}	3.0	0.5
P_{O_α}	6.3	1.8
P_{O_β}	7.7	4.5

Numbers were calculated by using rate constants listed in Table 1. Subscripts of P denote the state.

ties of occupancy of certain states in the gating scheme (*cf.*, Table 2) show that at low pH_{vac} dwelling in the C_1 state is markedly increased. The probability to attain the burst state (given by the occupancy of C_2 as a prerequisite) is at pH_{vac} 5.1 only 14% of that at pH_{vac} 7.3. This suggests that protonation is involved in the transition $C_1 \leftrightarrow C_2$. A significant effect of pH_{vac} 5.1 is seen in the backward transition $C_2 \rightarrow C_1$ (with the rate k_{21}, *cf.*, Table 1) which increased to a value 10-fold that of k_{21} at pH_{vac} 7.3. Thus, H^+ should operate on state C_2, inhibiting the entrance into a burst by increasing the probability to return into the inactive state C_1:

$$C_1 \underset{k_{21}}{\overset{k_{12}}{\rightleftharpoons}} C_2 \underset{k_{32}}{\overset{k_{23}}{\rightleftharpoons}} C_3 \underset{k_{\alpha 3}}{\overset{k_{3\alpha}}{\rightleftharpoons}} O_\alpha \underset{k_{\beta\alpha}}{\overset{k_{\alpha\beta}}{\rightleftharpoons}} O_\beta \qquad \text{(Scheme II)}$$

H^+

The analysis of transition rates presented here is based on the model of a Markov process, i.e., maxi-K channels switch independently of each other. How does this assumption cope with the recent report by Draber, Schultze and Hansen (1993) who described the activation of those channels to be cooperative in an ensemble? The application of such a cooperative model appears to be reasonable when channel clusters are recorded. Clusters may be found shortly after an exocytotic occurrence, when a dictyosomal vesicle with its membrane loaded with the respective channel protein had fused into the tonoplast. In cases of low population density (1–4 channels per μm^2) cooperativity cannot be acknowledged. Therefore, the assumption of independent channel switching in patches containing only a few channel copies appears to be reasonable.

The shift in activating voltage at low pH_{vac} suggests that a voltage sensor is involved in the gating process of the Characean maxi-K channel. This, in turn, requires a dislocation of charged residues in the channel protein to evoke a conformational modification required for the attainment of a conductant state. In *Shaker* K^+ channels, such a mechanism has been demonstrated by Larsson et al. (1996), showing that the highly charged transmembrane domain S4 almost completely moves through the membrane. With the cloning of *slo* channels (Atkinson, Robertson & Ganetzky, 1991; Adelman et al., 1992; Butler et al., 1993), it recently became apparent that animal maxi-K channels also contain an S4 domain. This prediction was supported by Cui, Cox and Aldrich (1997) by patch clamp experiments on the cloned *mslo* channel, contradicting the former suggestion by Moczydlowski and Latorre (1983) that voltage dependence of the maxi-K channel would reside in Ca^{2+} binding. To date, there are no data available about the molecular structure of the Characean maxi-K channel, hence, a structural interpretation can only be speculative. Suppose that the Characean K^+ channel protein also possesses a voltage sensor (S4-like) domain and accompanying transmembrane domains that carry negatively charged residues thought to stabilize the voltage-induced displacement of the sensor by electrostatical interaction (in S4: Papazian et al., 1995; Larsson et al., 1996), then part of those negatively charged residues could be accessible for H^+. As a result of neutralization, a relief in maneuverability of the voltage sensor could be expected which allowed a displacement by application of low electrical energy. In this respect, the rate k_{21} could reflect a weakness of the sensor state, hence, the transitions between C_1 and C_2 might be attributed to voltage sensor-mediated (de)activation of the channel. The approximately 50% increased forward rate $k_{3\alpha}$ and the 25–50% reduced backward rates $k_{\beta\alpha}$ and $k_{\alpha 3}$ could be sought in the gates residing in the pore region (*cf.*, Laver, 1990, Fig. 7 therein).

An acidic pH of about 5 has been determined previously to prevail in the vacuolar compartment (Spanswick & Miller, 1977; Mimura & Kirino, 1984; Moriyasu et al., 1984*a*), i.e., the effect of low pH_{vac} upon kinetics and activating voltage are reflecting natural conditions. Supplementing previous investigations with

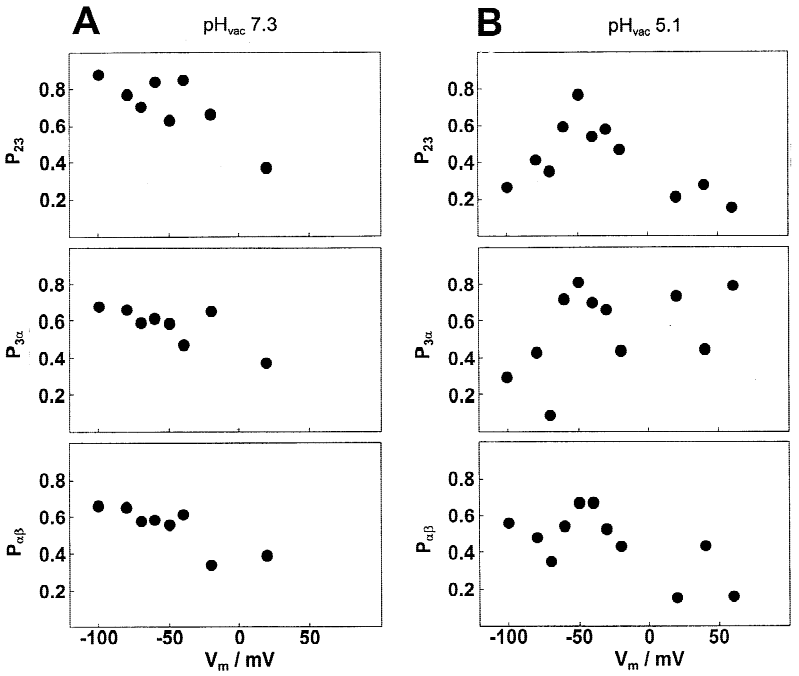

Fig. 10. Voltage-dependent probabilities of channel states to decay in forward (towards the open state) or backward direction (towards the closed state), respectively, as a function of membrane voltage at pH_{vac} 7.3 (*A*) or 5.1 (*B*) of the K^+ channel. A 5-state gating model was underlying this evaluation (*see* text). Transition probabilities were determined as the ratio between distinct forward transition rates out of a certain state and the sum of backward and forward transition rates leading from this state.

these results it is suggested that pH_{vac} largely controls the kinetics and, in particular, voltage sensitivity of the tonoplast-resident K^+ channel. In the case of cytosolic regulation, the effect of Ca^{2+}_{cyt} might be of greater importance than that of H^+_{cyt} because cytosolic acidification in a range of $\Delta pH_{cyt} \cong 1$ is rather unlikely, whereas Ca^{2+}_{cyt} increase to a μM range during an action potential is suggested to activate tonoplast-resident Cl^- and K^+ channels (Williamson & Ashley, 1982; Kikuyama & Tazawa, 1983; for review *see* Shimmen et al., 1994).

I am grateful to Dr. Ulf-Peter Hansen (Institute of Applied Physics, University of Kiel, Germany) for making the target fit program available to me, and also to his group, especially Maike Keunecke, who patiently introduced and guided me through the software. I thank Dr. S. Bauer for performing Scanning Electron Microscopy on patch pipettes. Contribution of helpful comments on the manuscript by Drs. A. Baumann, S. Frings, D. Gradmann, U.P. Hansen, R. Seifert, and G. Thiel is gratefully acknowledged. Furthermore, I have to thank Dr. U.B. Kaupp for support.

References

Adelman, J.P., Shen, K.Z., Kavanaugh, M.P., Warren, R.A., Wu, Y.N., Lagrutta, A., Bond, C.T., North, R.A. 1992. Calcium-activated potassium channels expressed from cloned complementary DNAs. *Neuron* **9:**209–216

Atkinson, N.S., Robertson, G.A., Ganetzky, B. 1991. A component of calcium-activated potassium channels encoded by the *Drosophila slo* locus. *Science* **253:**551–555

Barrett, J.N., Magleby, K.L., Pallotta, B.S. 1982. Properties of single calcium-activated potassium channels in cultured rat muscle. *J. Physiol.* **331:**211–230

Bell, J.E., Miller, C. 1984. Effects of phospholipid surface charge on ion conduction in the K^+ channel of sarcoplasmic reticulum. *Biophys. J.* **45:**279–287

Bertl, A., Gradmann, D. 1987. Current-voltage relationships of potassium channels in the plasmalemma of *Acetabularia. J. Membrane Biol.* **99:**41–49

Blatz, A.L., Magleby, K.L. 1987. Calcium-activated potassium channels. *Trends Neurosci.* **10:**463–467

Blunck, R., Kirst, U., Rießner, T., Hansen, U.-P. 1998. How powerful is the dwell-time analysis of multi-channel records? *J. Membrane Biol.* **165:**19–35

Butler, A., Tsunoda, S., McCobb, D.P., Wei, A., Salkoff, L. 1993. *mslo*, a complex mouse gene encoding 'maxi' calcium-activated potassium channels. *Science* **261:**221–224

Cecchi, X., Wolff, D., Alvarez, O., Latorre, R. 1987. Mechanisms of Cs^+ blockade in a Ca^{2+}-activated K^+ channel from smooth muscle. *Biophys. J.* **52:**707–716

Christensen, O., Zeuthen, T. 1987. Maxi K channels in leaky epithelia are regulated by intracellular Ca^{2+}, pH and membrane potential. *Pfluegers Arch.* **408:**249–259

Cook, D.L., Ikeuchi, M., Fujimoto, W.Y. 1984. Lowering of pH_i inhibits Ca^{2+}-activated K^+ channels in pancreatic B-cells. *Nature* **311:**269–271

Cui, J., Cox, D.H., Aldrich, R.W. 1997. Intrinsic voltage dependence and Ca^{2+} regulation of *mslo* large conductance Ca-activated K^+ channels. *J. Gen. Physiol.* **109:**647–673

Davies, J.M. 1997. Vacuolar energization: pumps, shunts and stress. *J. Exp. Bot.* **48:**633–641

Davies, J.M., Rea, P.A., Sanders, D. 1991. Vacuolar proton-pumping pyrophosphatase in *Beta vulgaris* shows vectorial activation by potassium. *FEBS Lett.* **278:**66–68

Draber, S., Schultze, R., Hansen, U.-P. 1993. Cooperative behavior of K^+ channels in the tonoplast of *Chara corallina. Biophys. J.* **65:**1553–1559

Eisenman, G., Latorre, R., Miller, C. 1986. Multi-ion conduction and

selectivity in the high-conductance Ca^{++}-activated K^+ channel from skeletal muscle. *Biophys. J.* **50:**1025–1034

Findlay, I. 1984. A patch-clamp study of potassium channels and whole-cell currents in acinar cells of the mouse lacrimal gland. *J. Physiol.* **350:**179–195

Findlay, G.P., Hope, A.B. 1964. Ionic relations of cells of *Chara australis.* VII. The separate electrical characteristics of the plasmalemma and tonoplast. *Aust. J. Biol. Sci.* **17:**62–77

Hamill, O.P., Marty, A., Neher, E., Sakmann, B., Sigworth, F.J. 1981. Improved patch-clamp techniques for high-resolution current recording from cells and cell-free membrane patches. *Pfluegers Arch.* **391:**85–100

Hansen, U.P., Keunecke, M., Blunck, R. 1997. Gating and permeation models of plant channels. *J. Exp. Bot. Special Issue* **48:**365–382

Hayama, T., Nakagawa, S., Tazawa, M. 1979. Membrane depolarization induced by transcellular osmosis in internodal cells of *Nitella flexilis. Protoplasma* **98:**73–90

Hedrich, R., Kurkdjian, A., Guern, J., Flügge, U.I. 1989. Comparative studies on the electrical properties of the H^+-translocating ATPase and pyrophosphatase of the vacuo-lysosomal compartment. *EMBO J.* **8:**2835–2841

Hinkley, D.H. 1970. Inference about the change-point in a sequence of random variables. *Biometrika* **57:**1–17

Katsuhara, M., Kuchitsu, K., Takeshige, K., Tazawa, M. 1989. Salt stress-induced cytoplasmic acidification and vacuolar alkalization in *Nitellopsis obtusa* cells. *Plant Physiol.* **90:**1102–1107

Kikuyama, M., Tazawa, M. 1983. Transient increase of intracellular Ca^{2+} during excitation of tonoplast-free *Chara* cells. *Protoplasma* **117:**62–67

Kume, H., Takagi, K., Satake, T., Tokuno, H., Tomita, T. 1990. Effects of intracellular pH on calcium-activated potassium channels in rabbit tracheal smooth muscle. *J. Physiol.* **424:**445–457

Larsson, H.P., Baker, O.S., Dhillon, D.S., Isacoff, E.Y. 1996. Transmembrane movement of the *Shaker* K^+ channel S4. *Neuron* **16:**387–397

Latorre, R., Miller, C. 1983. Conduction and selectivity in potassium channels. *J. Membrane Biol.* **71:**11–30

Laurido, C., Candia, S., Wolff, D., Latorre, R. 1991. Proton modulation of Ca^{2+}-activated K^+ channel from rat skeletal muscle incorporated into planar bilayers. *J. Gen. Physiol.* **98:**1025–1043

Laver, D.R. 1990. Coupling of K^+-gating and permeation with Ca^{2+} block in the Ca^{2+}-activated K^+ channel in *Chara australis. J. Membrane Biol.* **118:**55–67

Laver, D.R., Cherry, C.A., Walker, N.A. 1997. The actions of calmodulin antagonists W-7 and TFP and of calcium on the gating kinetics of the calcium-activated large conductance potassium channel of the *Chara* protoplasmic drop: a substate-sensitive analysis. *J. Membrane Biol.* **155:**263–274

Laver, D.R., Fairley, K.A., Walker, N.A. 1989. Ion permeation in a K^+ channel in *Chara australis:* direct evidence for diffusion limitation of ion flow in a maxi-K channel. *J. Membrane Biol.* **108:**153–164

Laver, D.R., Walker, N.A. 1987. Steady-state voltage-dependent gating and conduction kinetics of single K^+ channels in the membrane of cytoplasmic drops of *Chara australis. J. Membrane Biol.* **100:**31–42

Laver, D.R., Walker, N.A. 1991. Activation by Ca^{2+} and block by divalent ions of the K^+ channel in the membrane of cytoplasmic drops from *Chara australis. J. Membrane Biol.* **120:**131–139

Lühring, H. 1986. Recording of single K^+ channels in the membrane of cytoplasmic drops of *Chara australis. Protoplasma* **133:**19–28

Magleby, K.L., Pallotta, B.S. 1983. Calcium dependence of open and shut interval distributions from calcium-activated potassium channels in cultured rat muscle. *J. Physiol.* **344:**585–604

Marty, A. 1983. Ca^{2+}-dependent K^+ channels with large unitary conductance. *Trends Neurosci.* **6:**262–265

Matthew, J.B. 1985. Electrostatic effects in proteins. *Ann. Rev. Biophys. Chem.* **14:**387–417

Mimura, T., Kirino, Y. 1984. Changes in cytoplasmic pH measured by ^{31}P-NMR in cells of *Nitellopsis obtusa. Plant Cell Physiol.* **25:**813–820

Moczydlowski, E., Latorre, R. 1983. Gating kinetics of Ca^{2+}-activated K^+ channels from rat muscle incorporated into planar lipid bilayers: evidence for two voltage-dependent Ca^{2+}-binding reactions. *J. Gen. Physiol.* **82:**511–542

Moriyasu, Y., Shimmen, T., Tazawa, M. 1984*a*. Electric characteristics of the vacuolar membrane of *Chara* in relation to pH_v regulation. *Cell Struct. Funct.* **9:**235–246

Moriyasu, Y., Shimmen, T., Tazawa, M. 1984*b*. Vacuolar pH regulation in *Chara corallina. Cell Struct. Funct.* **9:**225–234

Okihara, K., Kiyosawa, K. 1988. Ion composition of the *Chara* internode. *Plant Cell Physiol.* **29:**21–25

Papazian, D.M., Shao, X.M., Seoh, S.A., Mock, A.F., Huang, Y., Wainstock, D.H. 1995. Electrostatic interactions of S4 voltage sensor in *Shaker* K^+ channel. *Neuron* **6:**1293–1301

Perutz, M.F. 1978. Electrostatic effects in proteins. *Science* **201:**1187–1191

Pottosin, I.I. 1990. Voltage- and Ca^{2+}-regulated K^+ channel in the tonoplast of Characean algae. *Studia biophysica* **138:**119–126

Pottosin, I.I., Andjus, P.R., Vucelic, D., Berestovsky, G.N. 1993. Effects of D_2O on permeation and gating in the Ca^{2+}-activated potassium channel from *Chara. J. Membrane Biol.* **136:**113–124

Press, W.H., Flannery, B.P., Teukolsky, S.A., Vetterling, W.T. 1987. Numerical Recipes. The Art of Scientific Computing. Cambridge University Press, Cambridge, New York, New Rochelle, Melbourne, Sidney

Raghavan, V., Lambright, D.G., Boxer, S.G. 1989. Electrostatic interactions in wild-type and mutant recombinant human myoglobins. *Biochemistry* **28:**3771–3781

Rea, P.A., Poole, R.J. 1986. Chromatographic resolution of H^+-translocating pyrophosphatase from H^+-translocating ATPase of higher plant tonoplast. *Plant Physiol.* **81:**126–129

Reeves, M., Shimmen, T., Tazawa, M. 1985. Ionic activity gradients across the surface membrane of cytoplasmic droplets prepared from *Chara australis. Plant Cell Physiol.* **26:**1185–1193

Reid, R.J., Smith, F.A. 1988. Measurements of the cytoplasmic pH of *Chara corallina* using double-barrelled pH micro-electrodes. *J. Exp. Bot.* **39:**1421–1432

Sakano, K., Tazawa, M. 1986. Tonoplast origin of the membrane of cytoplasmic droplets prepared from *Chara* internodal cells. *Protoplasma* **131:**247–249

Schultze, R., Draber, S. 1993. A nonlinear filter algorithm for the detection of jumps in patch-clamp data. *J. Membrane Biol.* **132:**41–52

Schulz-Lessdorf, B., Hedrich, R. 1995. Protons and calcium modulate SV-type channels in the vacuolar-lysosomal compartment—channel interaction with calmodulin inhibitors. *Planta* **197:**655–671

Sharp, K.A., Honig, B. 1990. Electrostatic interactions in macromolecules: theory and application. *Ann. Rev. Biophys. Chem.* **19:**301–332

Shimmen, T., MacRobbie, E.A.C. 1987. Demonstration of two proton translocating systems in tonoplast of permeabilized *Nitella* cell. *Protoplasma* **136:**205–207

Shimmen, T., Mimura, T., Kikuyama, M., Tazawa, M. 1994. Characean cells as a tool for studying electrophysiological characteristics of plant cells. *Cell Struct. Funct.* **19:**263–278

Shimmen, T., Nishikawa, S. 1988. Studies on the tonoplast action potential of *Nitella flexilis. J. Membrane Biol.* **101:**133–140

Smith, F.A., Raven, J.A. 1979. Intracellular pH and its regulation. *Annu. Rev. Plant Physiol.* **30:**289–311

Spanswick, R.M., Miller, A.G. 1977. Measurement of the cytoplasmic pH in *Nitella translucens.* Comparison of the values obtained by microelectrode and weak acids methods. *Plant Physiol.* **59:**664–666

Takeshige, K., Hager, A. 1988. Ion effects on the H^+-translocating adenosine triphosphatase and pyrophosphatase associated with the tonoplast of *Chara corallina. Plant Cell Physiol.* **29:**649–657

Takeshige, K., Tazawa, M., Hager, A. 1988. Characterization of the H^+-translocating adenosine triphosphatase and pyrophosphatase of vacuolar membranes isolated by means of a perfusion technique from *Chara corallina. Plant Physiol.* **86:**1168–1173

Tominaga, Y., Shimmen, T., Tazawa, M. 1983. Control of cytoplasmic streaming by extracellular Ca^{2+} in permeabilized *Nitella* cells. *Protoplasma* **116:**75–77

Tyerman, S.D., Findlay, G.P. 1989. Current-voltage curves of single Cl^- channels which coexist with two types of K^+ channel in the tonoplast of *Chara corallina. J. Exp. Bot.* **40:**105–117

Tyerman, S.D., Terry, B.R., Findlay, G.P. 1992. Multiple conductances in the large K^+ channel from *Chara corallina* shown by a transient analysis method. *Biophys. J.* **61:**736–749

Walker, N.A., Smith, F.A. 1975. Intracellular pH in *Chara corallina* measured by DMO distribution. *Plant Sci. Lett.* **4:**125–132

Williamson, R.E., Ashley, C.C. 1982. Free Ca^{2+} and cytoplasmic streaming in the alga *Chara. Nature* **296:**647–651

Yang, A.-S., Barry H. 1994. Structural origins of pH and ionic strength effects on protein stability. Acid denaturation of sperm whale apomyoglobin. *J. Mol. Biol.* **273:**602–614

Yang, A.-S., Honig, B. 1992. Electrostatic effects on protein stability. *Curr. Opin. Struct. Biol.* **2:**40–45

Yang, A., Honig, B. 1993. On the pH dependence of protein stability. *J. Mol. Biol.* **231:**459–474

Yellen, G. 1984. Ionic permeation and blockade in Ca^{2+}-activated K^+ channels of bovine chromaffin cells. *J. Gen. Physiol.* **84:**157–186